



Poly N-(2-aminoethyl) acrylamide-NiO composite as novel efficient photocatalyst for desulfurization of diesel fuel under visible-light irradiation

Usama A. Metwally ^{1*}, Asmaa S. Morshedy ², Ahmed M.A. El Naggar², Nour E.A. Abd el-satar ³, Emad A. Soliman ⁴, Ahmed I. Hashem ³



CrossMark

¹ Cairo oil refining company (CORC), Mostorod-Cairo, Egypt.

² Refining Division, Egyptian petroleum research institute (EPRI), 11727, Cairo, Egypt.

³ Chemistry Department, Faculty of Science, Ain Shams University, Egypt.

⁴ Advanced technology's and new materials insitute, City of scientific research and technology applications, New Borg El-arab city, 21934, Alexandria, Egypt.

Abstract

The disposal of sulfur compounds from fossil fuels in general and diesel fuels particularly has been stimulated worldwide due to their harmful environmental emissions during the combustion process. Several desulfurization techniques can be employed; however, photocatalytic desulfurization can be considered as the safest and cost-effective route to achieve such goal. This study introduces a novel hybrid photocatalyst made of coupling both NiO and poly-acrylamide based polymer. Such composite could have improved photo-luminance (PL) properties than that of pure NiO. Additionally, the combination of NiO (which is UV-active photocatalyst) with polymer could result in producing visible-light effective composite. These optical properties had progressively improved the photocatalytic desulfurization performance of this composite. It could attain a sulfur removal of 60 % from a diesel fuel fraction contains 12300 ppm of sulfur. This rate of sulfur removal could be counted as an extremely high and of obvious advancements in the field of diesel fuel desulfurization.

1. Introduction

Diesel fuel feedstocks usually contain a big number of various types sulfur compounds. The concentration of these compounds, in a certain fraction, is basically depending on the origin of the petroleum crude oil. Desulfurization of diesel fuel has increasingly gained importance since most of the countries, especially the developed ones, have implemented increased stringent legislation to regulate sulfur content of diesel fuel. Sulfur content in diesel fuels can play a key role as a main contributor to air pollution due to the emitted SO₂, during their combustion, along with particulate matter from vehicles [1-3]. Hydrodesulfurization (HDS) is the most commonly used method in petroleum refining industry to reduce the sulfur content of crude oil and its products where the sulfur in the organosulfur compounds is converted into H₂S via HDS catalysts under high temperature (up to 400°C) and high hydrogen pressure (up to 80 bar) [4]. Other desulfurization methods of diesel fuel such as

Oxidative desulfurization (ODS), Adsorptive desulfurization (ADS), Ultrasound assisted oxidative desulfurization (UAOD) and Photochemical oxidative desulfurization (PCOD) are considered as alternative technologies for desulfurization of diesel fuel fractions instead of HDS [5-8]. Both the economic and technological importance toward photocatalysts of desulfurization has increased considerably over the past decade. Photocatalytic desulfurization reaction with sunlight as an energy source is one of the promising methods and has been recently investigated as a new alternative technology for the deep desulfurization of fuel oils [9, 10]. So far, a number of photocatalysts, based on metals oxides such as NiO, have attracted a great attention due to their excellent photocatalytic performance in the process of photocatalytic desulfurization [11-13]. Alternative materials, such as polymeric carbon nitride, have been proposed as efficient photocatalysts for various processes [14]. Moreover, nano-structured

*Corresponding author e-mail: umetwally@gmail.com; (Usama A. Metwally).

Receive Date: 01 May 2021, Revise Date: 30 May 2021, Accept Date: 02 June 2021

DOI: 10.21608/EJCHEM.2021.74733.3681

©2021 National Information and Documentation Center (NIDOC)

photocatalysts modified with some polymers have been lately considered for photocatalytic applications. For instance, poly-pyrrole films containing TiO₂ nanoparticles exhibited higher photocatalytic activity than bare TiO₂ for the degradation of dyes under ultraviolet radiation [15-17]. In the current research work, a novel photocatalytic composite based on incorporation of NiO nanoparticles (as main photocatalytic sites) and poly acrylamide based polymer has been introduced. The performance of this photocatalyst toward the process of sulfur compounds removal is going to be investigated. Also, a comparison between the optical properties of both bare NiO and its sub-produced NiO-polymer composite is discussed through this study.

2. Experimental

Synthesis of the photocatalysts in the current study had obeyed two stages. The first one includes preparation of NiO particles while in the second these particles were combined with an organic compound (acrylamide based polymer).

2.1 Preparation of acrylamide polymer

In this step, propenoyl chloride was first prepared by adding acrylic acid (1.4 g equal to 20 mmol) to 30mL of thionyl chloride. The obtained mixture was held under stirring and reflux for a time of three hours. The excess of thionyl chloride was evaporated via distillation to obtain the targeted structure. Subsequently, propenyl chloride (0.9 g = 10 mmol) had reacted with (10 mmol) of ethylene diamine in 10 mL dry benzene under vigorous stirring. This reaction was held for 10 min where the benzene was then decanted to obtain N-(2-aminoethyl) acrylamide (brown oily product). The melting point of as-synthesized compound was measured using an electric melting point apparatus (Camlab digital models SMP10). The structural characteristics of this structure was acquired and recorded via Fourier Transform Infrared (FTIR) device model Pye Unicam SP-3-300 infrared spectrophotometer (Germany) using potassium bromide (KBr) disks method. After confirming the produced structure, it was forwarded to a polymerization stage, as described by Bakr et al [18].

2.2 Synthesis of NiO nanoparticles

Nickel oxide nanoparticles were prepared by the chemical precipitation technique as reported in [19,

20]. Specifically, 0.1 M solution of nickel nitrate hexahydrate [Ni (NO₃)₂.6H₂O] was prepared and heated up to 70 °C. Then, drop-wise addition of ammonia solution (30 %) had taken place in order to extract nickel metal from its precursor in the form of nickel hydroxide. The precipitated particles were next filtered and washed by double distilled-water for several times. After the washing step, they were forwarded for drying for 3 h inside an electrical oven at 100 °C. Nickel hydroxide particles were afterward calcined at 500 °C for 4 h to release their molecular water to ultimately produce NiO nanoparticles.

2.2.1 Characterization of NiO particles

The structural properties of NiO were verified through both X-ray diffraction (XRD) Pan Analytical diffractometer version X'Pert Pro (Germany) and Fourier Transform Infrared (FTIR) analyses using Infrared Spectrometer model Bruker Tensor 27 (Germany). Thermal behavior of the produced particles was picked via Thermal gravimetric analysis (TGA) technique using TA Instruments Q500 (USA) while their morphological look was obtained by transmission electron microscopy analysis (TEM) model JEM 2100 (JEOL, Japan). The optical characteristics for NiO nanoparticles were gained via both UV reflectance spectrophotometer model V-570 manufactured by JASCO (Japan) and photo-luminance (PL) techniques using Spectrofluorometer, model Jasco FP-6500, Japan.

2.3 Photocatalytic desulfurization

After both the polymer and NiO were prepared, they were mixed together through mechanical suspension using ethanol at 50 °C to produce a composite for use as a photocatalyst. The obtained structure was then utilized for the process of photocatalytic desulfurization of a diesel fuel feedstock (sulfur content of 12,500 ppm) from Cairo oil refining company with the following specification: density = 0.8475 g/cm³, flashpoint = 80 °C, pourpoint = 3 °C. The application started at the beginning by testing the efficiency of NiO nanoparticles, as a photocatalyst for sulfur compounds removal. This step was done under visible light at operating conditions of: 90 min and catalysts dose of 10 g/L. Then, the hybrid composite was tested against desulfurization of diesel fuel at the same operational conditions. The effect of metal oxide/polymer ratio, dose of the composite

photocatalyst and time of exposure to visible light radiation on the desulfurization process had been studied. Determination of sulfur content of the diesel fuel as well as the obtained product at each step of the diesel fuel refining (desulfurization) was performed using X-ray fluorescence (XRF) spectrophotometer model PANalytical Epsilon 1 (Netherlands). Sulfur removal percentage was calculated according to the following equation:

$$S \text{ removal } \% = (S_F - S_P) / S_F$$

where S_F is sulfur content of feedstock and S_P is the sulfur content of obtained products after desulfurization process

All the sulfur removal experiments were carried out in a batch system which is diagrammatically presented in figure 1. The desulfurization reaction was carried out in a glass double jacket vessel (component number 3) connected with a water circulator. The photocatalytic desulfurization system has been fitted with a source of visible light irradiation (component number 2) which is horizontally fixed on a distance of 20 cm from the glass double jacket.

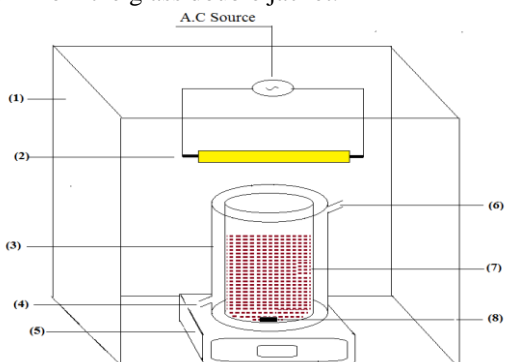


Figure1: Photocatalytic desulfurization set up fitted with irradiation source.

- | | |
|-------------------------|-------------------------|
| (1) Woody box | (2) Linear halogen lamp |
| (3) Glass double jacket | (4) Water inlet |
| (5) Magnetic stirrer | (6) Water outlet |
| (7) Diesel Feed | (8) Stirrer bar |

This light source in the above photocatalytic system was a Linear Halogen Lamp (LHL) manufactured by Sylvania Ltd and holds a Product EAN number 5410288217208. The design of utilized LHL during this research work is shown through figure 2

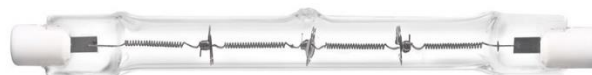


Figure2: Linear Halogen Lamp (LHL) of a power = 400 W

At first, both the NiO based photocatalyst and the feedstock (diesel fuel) were charged into the glass double jacket (a total capacity of 250 ml). Then, the whole system was then exposed to the irradiation source, in order to get the process started, and was kept under stirring at 500 rpm to properly disperse the catalyst particles within the feedstock.

3. Results and discussion

This research work introduces new advances in the field of photocatalytic desulfurization of petroleum diesel fuels. Particularly, a novel photocatalyst made through combination of nickel oxide nanoparticles and a poly-acrylamide structure is presented. The novelty of such study is based on coupling both organic and inorganic structures in a hybrid composite to act as an efficient photocatalyst. At the first place, the structural, thermal, and morphological characteristics of NiO, which possess the main photocatalytic sites, were determined. Then, its optical properties either as individual or couples with functionalized acrylamide monomer/ polymer had been studied.

3.1. Structural properties

The confirmation of obtaining particle of nickel oxide, during this study, had been carried out via the introduced XRD spectrum in Figure 3. Four sharp strong peaks, indicative to NiO, centered around 2θ of 39° , 44° , 62° and 75° could be obviously noticed through the displayed spectrum [21, 22]. The sharpness of the detected signals is referring to the formation of NiO particles as crystals. Moreover, the increased intensity of these signals is reflecting the high degree of crystallinity of the produced nickel oxide particles. The collected data from XRD analysis were then utilized to calculate the average crystal size of the presented NiO, via Scherer's equation. The average crystal size was found to be 39.5 nm, confirming the formation of NiO nanoparticles.

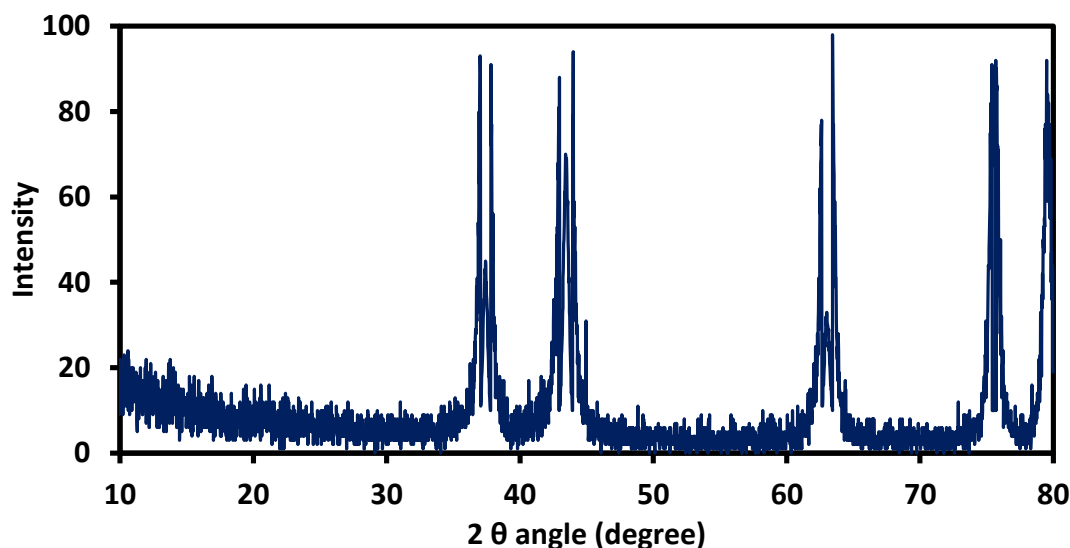


Figure 3: XRD pattern of the as-prepared nickel oxide nanoparticles

The structural characteristics of the nickel oxide particles had been further verified through the exhibited FTIR spectrum in Figure 4. Absorption band could be noticed at wave numbers of 670 cm^{-1} . The signal is assigned to stretching NiO band. On the other hands, a quite sharp intense absorption band could be

seen, through Figure 4, at wave number of 3680 cm^{-1} . This band can be attributed to OH groups that could be stuck [23] among the particles of NiO during their production from their corresponding hydroxide structure. The slightly present OH groups as attached to the obtained NiO crystals, in this study, had been confirmed via the next illustrated thermal properties.

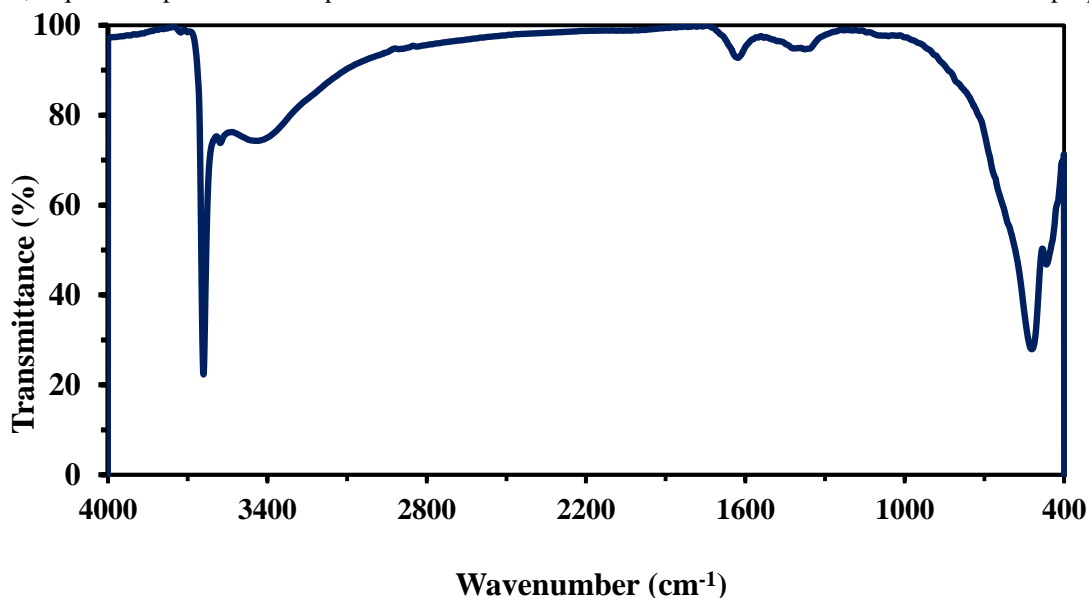


Figure 4: FTIR spectrum of nickel oxide nanoparticles

3.2 Thermal behaviour

The thermal behavior of the introduced NiO nanoparticles could be observed through the provided thermal gravimetric analysis – differential scanning calorimetry (TGA-DSC) spectra in Figure 5. A high level of thermal stability could be detected since an

overall weight loss of 2 Wt % could be observed up to a testing temperature of $800\text{ }^{\circ}\text{C}$.

Half of this weight loss could be noted at $100\text{ }^{\circ}\text{C}$ which had been accompanied with an exothermic peak in the shown DSC pattern. This peak is indicative to the release of adsorbed water molecules onto the NiO

nanoparticles [24]. Another peak, however an endothermic, could be noticed in this DSC analysis between 400 and 500 °C. This peak can be explained due to the exist remains of hydroxyl groups that could be convert to the oxide form at that temperature range [25]. This finding is of a good match with previously

given data in the FTIR spectrum, Figure 4. The limited percentages of weight loss as given by TGA analysis, Figure 5, could authenticate the nice thermal attitude of NiO nanoparticles since no phase changes or transition states could be noted.

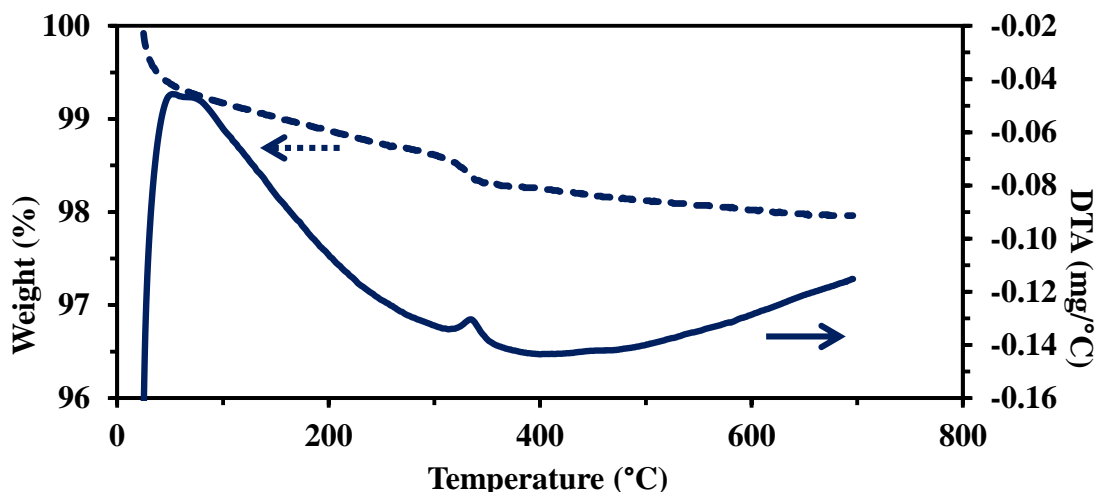


Figure 5: TGA-DTA profiles for the as-prepared nickel oxide nanoparticles

3.3 Morphological appearance

The inner morphological appearance of the as-prepared NiO nanoparticles is illustrated through the shown TEM micrograph, Figure 6. The presented morphology has been of a strong agreement with previously displayed XRD pattern. Specifically, nanoparticles of different shaped crystals had been detected in the provided TEM image. Spherical, tetrahedral, oval and rod-like crystals could be observed through the displayed image. No amorphous particles could be noticed through TEM micrograph which has been in a strong harmony with the XRD signals; showing high level of crystallinity for the tested specimen. TEM could also reveal high dispersity of NiO particles however some aggregates could be noticed at some spots along the sample. Generally, it could be stated that the morphology of the sample is mostly of a high uniformity but not completely smooth. The detected particles in TEM image could have different sizes ranged between 20 and nearly 70 nm. This once again could highly likely match to the calculated average crystal size (nearly 40 nm) by the XRD analysis.

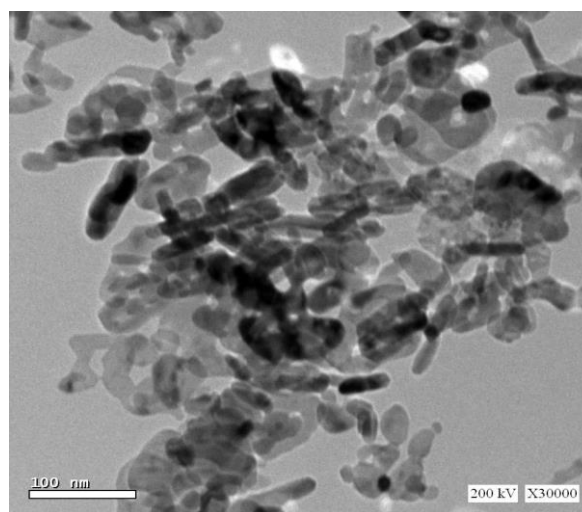


Figure 6: TEM micrograph for the as-synthesized Ni oxide nanoparticles

3.4 Optical properties

Before subjecting either the NiO or its composite with the poly acrylamide based polymer to the photocatalytic process, it was necessary to determine their optical characteristics in order to find out about their potential efficiency. Both UV reflectance and band gap measurements had been performed for the two structures, as exhibited in Figure 7.

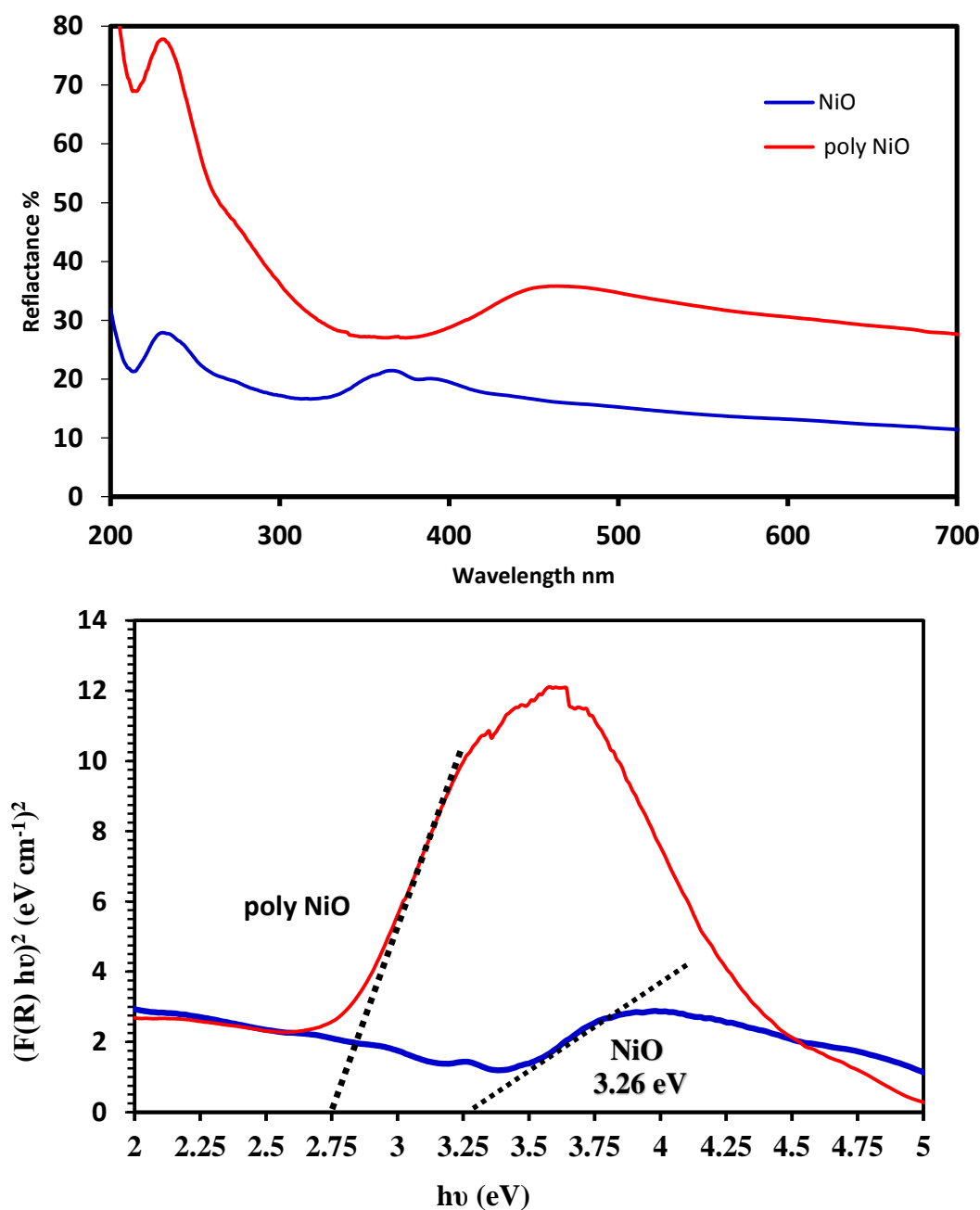


Figure 7: (a) UV reflectance (b) band gap of Ni oxide nanoparticles

It could be observed that the blank NiO had lied on the zone of UV-effective photocatalyst while the composite could show better effectiveness in the zone of UV-visible, this could obviously refer to a potential higher photocatalytic performance by the composite, compared to the blank NiO. The reduced band gap value for the composite than NiO is attributed to the incorporation of the polymer which is a structure of a high electron density. The presence of the polymer

electrons could in turn shift the valence band electrons of NiO to higher sub-energy level [26]. Therefore, the band gap value could be reduced to less than 3.25 in the case of the produced composite by mixing NiO and polymer.

The optical characteristics of NiO and its composites either with the acrylamide-based monomer or its sub-driven polymer had been further investigated via PL curves, as shown in Figure 8.

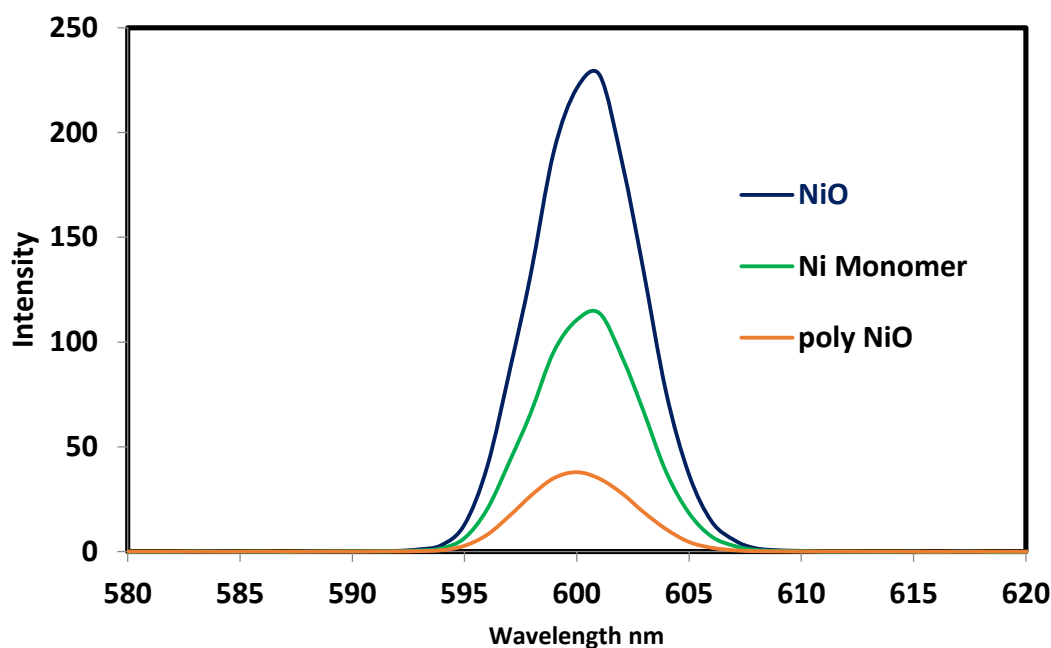


Figure 8: PL graphs for NiO and its composites with acrylamide based monomer and polymer

It can be explicitly seen that the composite which was made from NiO and polymer had presented the lowest PL value reflecting the highest potential of photocatalytic activity. On the other hand, the highest PL value could be observed for NiO which reveal the lowest possibility of photocatalytic performance among the three tested structures. The reduction of PL value in case of the two composites is explained by the interference between the electron's energy levels of both the organic sites and those of NiO. This intervention of energy levels could result in delay of recombination between the produced e-hole pairs in NiO during exposure to photo-illumination [27]. Therefore, increased potentiality for photocatalytic attacks by the photocatalytic sites toward the designated substrates (sulfur compounds) can undertake. The lower photocatalytic performance for the composite made of monomer than that of the containing polymer is referred to the higher intensity

of electrons in the latter structure than in case of the first one.

3.5 Photocatalytic desulfurization activity

After the full characteristics of NiO were obtained, the sub-obtained composite of poly N-(2-aminoethyl) acrylamide-NiO, by physical suspension, was then forwarded as a photocatalyst to the process of diesel fuel desulfurization. In this stage the effect of different operational parameters such effect of catalyst composition, reaction times and the employed dose of photocatalyst were investigated. However before testing these parameters, the effect of using NiO as individual and as coupled with N-(2-aminoethyl) acrylamide monomer as well as its polymer, as photocatalysts, on the desulfurization process was carried out. Table 1, illustrates the obtained desulfurization levels by the three aforementioned photocatalysts with a full statement for the employed operating conditions.

Table 1: Operational variables and desulfurization percentages by three different compositions

No.	Catalyst	Organic %	NiO %	Radiation time (min)	Catalyst dose (g/L)	S Removal %
1	NiO	-	100	90	10	16.08
2	N-(2-aminoethyl) acrylamide + NiO	50	50	90	20	19.38
3	poly N-(2-aminoethyl) acrylamide + NiO	50	50	90	20	58.36

It could be observed that the introduction of NiO alone as a photocatalyst could show the lowest photocatalytic desulfurization percentage, 16 Wt %. This limited level of sulfur removal can be attributed to the band gap value of NiO [28], as discussed in section 3.4. Particularly, NiO had shown effective performance in the region of UV region while the displayed desulfurization activities (Table 1) were carried out under effect of visible light irradiation. The combination of NiO with the organic structure (**N-(2-aminoethyl) acrylamide monomer**) could slightly enhance the sulfur removal percentage. This improvement in activity is due to the incorporation of NiO (the photocatalytic sites) with other supportive electron provider systems [29]. Therefore, the PL emission of the obtained composite (NiO + organic part), Figure 8, could be decreased leading to a modified photocatalytic activity. The subsequent use of NiO as a composite with **poly N-(2-aminoethyl) acrylamide** could massively elevate the photocatalytic desulfurization percentage to reach three folds of the obtained value via using its monomer. This observable enhancement could be generally referred to the overall improvement of optical properties of NiO-polymer composite [30]. Specifically, it showed the lowest PL value among the three tested photocatalysts as well as it showed an effective activity in the zone of UV-visible irradiation. Thus, the photocatalytic efficiency of this composite could be significantly taken to up levels. The improvement of optical properties can be explained by the increase of electron density, within the presented composite, by incorporation of the organic part (polymer) with NiO. This increment of density could, in turn, result in reducing the band gap and increase PL quality of NiO due to overlap of its electrons in outer most shell with the electronic systems of organic part [27, 31]. However in order to get sure of the photocatalytic performance of the presented composite (polymer and NiO), it has been necessary to repeat the desulfurization process at same conditions while in absence of light illumination (in dark). A maximum sulfur removal percentage of 14 % could be observed by the composite which can be attributed to its adsorption capability. Therefore, the observed desulfurization level above the latter percentage can be explained due to the photocatalytic performance of the composite.

3.5.1 Effect of catalysts composition on sulfur removal

By completing the former level of investigation in this research work, **NiO-polyN-(2-aminoethyl) acrylamide composite** was selected to perform the coming stages since it showed the highest percentage of sulfur removal. In the current stage, the impact of varying the ratio of **polyN-(2-aminoethyl) acrylamide to NiO** on the process of diesel fuel desulfurization had been studied. Figure 9 exhibit the levels of diesel fuel desulfurization as well as the operating conditions at which the sulfur elimination process was executed. It could be noticed that the increase of polymer content in the composite had been accompanied with a notable increase in sulfur removal percentage until an equal ratio of polymer to NiO could be reached. This elevation in desulfurization levels can be attributed to the improvements of optical properties of the introduced photocatalyst by increasing the content, by weight, of the organic sites [32]. Specifically, the band gap and PL values could be reduced due to the overlap between the electron clouds of the different components of the composite [33]. Hence, the photocatalytic performance of this composite could be obviously enhanced. On the other hand, the increase of polymer to NiO, in the composite, to above 1 could be associated with decreases in desulfurization levels. These declines could be referred to decrease in the number of effective photocatalytic sites [34] within the composite. Thus, limited attacks, by the photocatalyst, toward the sulfur compounds in diesel fuel could take place.

3.5.2 Effect of photocatalyst dose on desulfurization process

By the end of previous stage, the composition of photocatalyst which contained equal weight percents of polymer and NiO was chosen to implement the current stages of this research study. Figure 10 and Table 2 discuss the percentages of sulfur disposal and the operating parameters of the treatment process respectively.

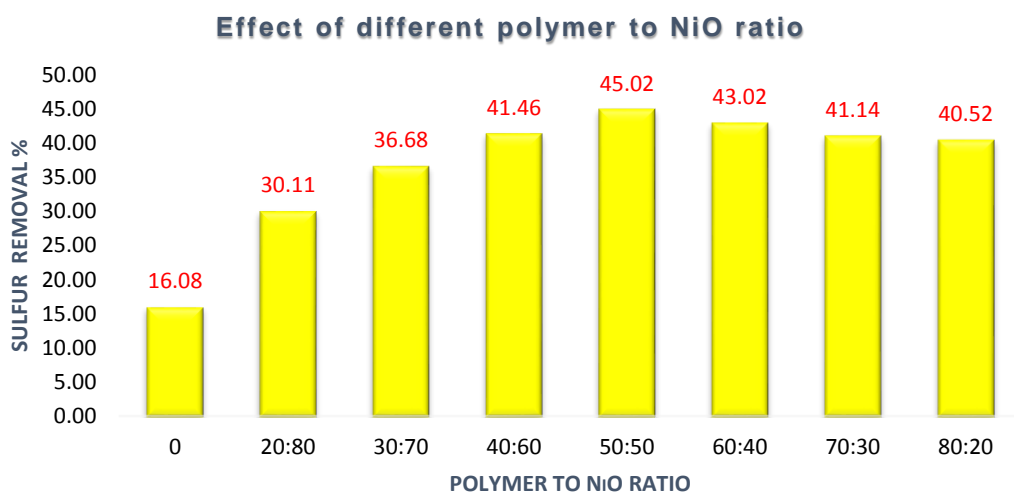


Figure 9: Effect of polymer content on the photocatalytic performance during process of sulfur removal from a petroleum diesel fuel fraction

Table 2: Operational conditions and sulfur removal percentages by polyN-(2-aminoethyl) acrylamide-NiO composites at different doses

No.	polymer N-(2-aminoethyl) acrylamide +NiO Catalyst		Radiation time (min)	Catalyst dose (g/L)	S Removal %
	Polymer %	NiO %			
1	50	50	90	10	45.02
2	50	50		20	58.36
3	50	50		30	39.84

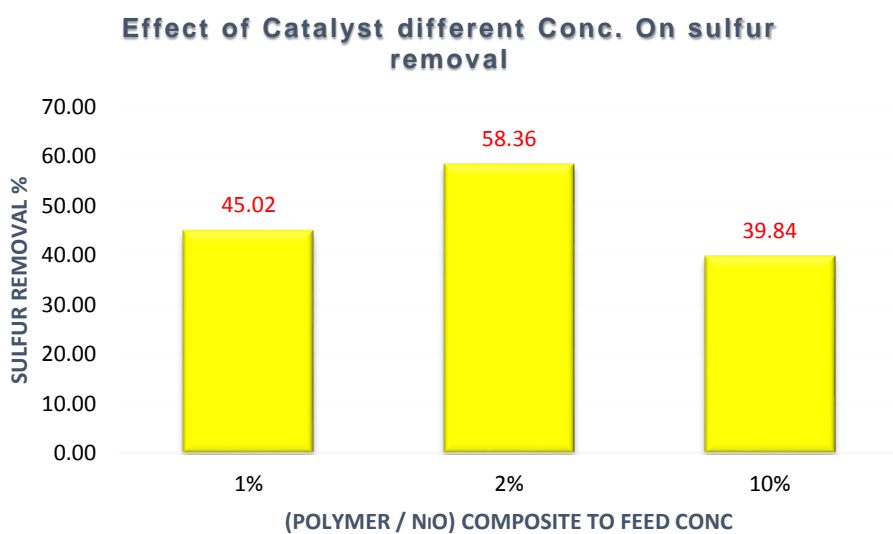


Figure 10: Effect of photocatalyst dose on the process of sulfur removal from a petroleum diesel fuel fraction

The increase of the photocatalysts dose from 10 to 20 g/L could remarkably elevate the level of desulfurization by approximately 60 Wt %. This increment is of course due to the increase in number of photocatalytic sites by increasing the dose of the introduced composite [35]. However, the increase of dose from 20 to 30 g/L could be joined by a noticeable decrease in the percentage of sulfur compounds removal. The observed drop in sulfur removal percentage can be due to the scattering of visible light photons among an increased number of the photocatalyst particles [36]. Therefore, a reduced photocatalytic activity could be attained by the introduced composite. In a conclusion to this stage, a photocatalyst amount of 20 g/L had been picked as the

optimum dose to perform the following stage of current study.

3.5.3 Effect of reaction time on sulfur removal process

In the current stage, the effect of different operating times on the quality of sulfur removal process had been investigated, as illustrated through both Table 3 and Figure 11. The displayed data could reveal that the time increase from 60 to 90 min could enhance the desulfurization level by nearly 25 %. This observation can be explained by increasing the probability of interaction between the effective sites of the photocatalyst and the substrate [26] (sulfur compounds in diesel fuel) by increase of reaction time.

Table 3: Variables of desulfurization process and sulfur removal percentages by polyN-(2-aminoethyl) acrylamide-NiO composites at different operating times

No.	polymer N-(2-aminoethyl) acrylamide +NiO Catalyst		Radiation time (min)	Catalyst dose (g/L)	S Removal %
	Polymer %	NiO %			
1	50	50	60	20	33.06
2	50	50	90	20	58.36
3	50	50	120	20	30.06
4	50	50	150	20	9.42

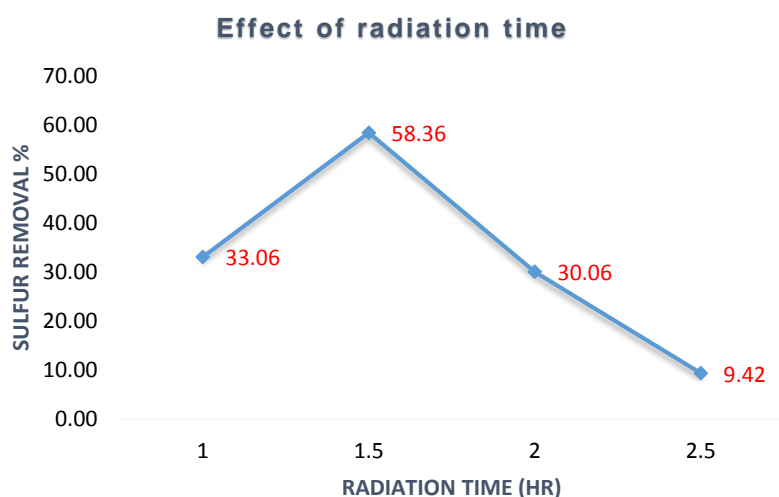


Figure 11: Effect of operational time on the process of sulfur removal from a petroleum diesel fuel fraction

The consequent increase of the processing time to 120 min had reduced the sulfur removal by nearly 28 %. This was followed by a further reduction of approximately 20 % in the desulfurization level as the operational time had increased to 150 min. The continuous decline of sulfur removal percentages

could be attributed to the coverage of catalysts surface by a mono-layer of adsorbate [37, 38], sulfur compounds, as the time went over 90 min. Therefore, limited photocatalytic activities could be achieved after a certain time of processing.

3.5.4 Reusability of the composite photocatalyst

In order to further investigate the reliability of the introduced composite for the desulfurization process, the spent photocatalyst was collected and regenerated via a consequence of washing via proper solvents (benzene/ methanol mixture), and then by ethanol. The recovered and dried composite was then introduced to the process of diesel fuel desulfurization at the pre-determined optimum conditions from the prior stages. The recovered photocatalyst could show a nearly stable sulfur removal percentage of 57 % over five rounds of reusability.

4. Conclusion

Nanoparticles of nickel oxide were prepared via chemical precipitation method and their structural characteristics were verified via both XRD and FTIR. Confirming the presence of nano-scaled particles could be acquired via both XRD particle size measurements and TEM analysis. The prepared nanoparticles had presented high good thermal stability and attitude, as collected from TGA test. These nanoparticles could show high value of band gap and quite good PL emission however their sub-obtained composite with functionalized poly-acrylamide could have strongly improved optical properties. Both NiO, as individual, and its composite with the polymer had exhibited a photocatalytic desulfurization activity under the effect of visible light irradiation. Nevertheless, the composite structure could display nearly four times the obtained activity by NiO. The composite of NiO and polymer of acrylamide derivatives could attain a sulfur removal percentage of 60 Wt % using a feedstock contain 12500 ppm, as a sulfur content. This percentage of desulfurization could be obtained at operating conditions of: 90 min, 20 g/L and photocatalyst composition of 1:1, by weight, polymer to NiO. The observed sulfur removal % by the presented composite during this study is counted as extremely high in terms of pure photocatalytic route with no further assistance. The corresponding photocatalysts, as reported in literature, in similar application (desulfurization of real diesel fuel sample) could achieve maximum desulfurization percentages ranged between 25-30 %.

References

- 1) A. I. Zahran, A. M. A. El Naggar, W. A. Aboutaleb, M. A. Sayed, H. S. Ahmed, M. A. Mekewi, Enhancement of heavy vacuum gas oil desulfurization via using developed catalyst based
- 2) H. A. El Sayed, A. M. A. El Naggar, B. H. Heakel, N. E. Ahmed, S. Said, A. A. Abdel-Rahman, Deep catalytic desulphurization of heavy gas oil at mild operating conditions using self-functionalized nanoparticles as a novel catalyst. *Fuel*, **209**, 127-131 (2017)
- 3) K. R. Balinge, A. G. Khiratkar, M. Krishnamurthy, D. S. Patle, K. K. Cheralathan, P. R. Bhagat, Deep-desulfurization of the petroleum diesel using the heterogeneous carboxyl functionalized poly-ionic liquid. [Resource-Efficient Technologies](#), **2**(1), S105-S113 (2016).
- 4) A. M. A. El Naggar, H. A. El Sayed, A. A. Salem, N. E. A. Abd El-Sattar, A new approach for catalytic production of ultra-low sulfur diesel fuel using binary composed catalysts consisting of cobalt nanoparticles. *industrial and engineering chemistry research (ACS)*, **59**, 7277-7290 (2020).
- 5) A. M. Dehkordi, Z. Kiaei, M. A. Sobati, Oxidative desulfurization of simulated light fuel oil and untreated Kerosene. *Fuel Processing Technology*, **90**, 435-445 (2009).
- 6) W. Qin, L. Xiao-yi*, Z. Rui, L. Chao-jun, L. Xiao-jun, Q. Wen-ming, Z. Liang, L. Li-cheng, Preparation of polystyrene-based activated carbon spheres and their adsorption of dibenzothiophene. *New Carbon Materials*, **24** (1), 55-60 (2009).
- 7) G. Zhang, F. Yu, R. Wang, Research advances in oxidative desulfurization technologies for the production of low sulphur fuel oils. *Petrol. Coal*, **51**, 196-207 (2009).
- 8) D. S. Zhao, L. F. Tang, Z. M. Sun, Study on photosensitized oxidative desulfurization of thiophene by riboflavin. *Fuel. Chem. Technol*, **36**, 161-164 (2008).
- 9) J. Zhang, D. S. Zhao, J. L. Wang, L. Y. Yang, Photocatalytic oxidation of dibenzothiophene using TiO₂ . charcoal. *Sci*, **44**, 3112-3117 (2009).
- 10) A. M. A. El Naggar, M. S. Mostafa, M. T. Zaky, New trend for the pour point depression of a waxy petroleum fraction with in-situ desulphurization using (O₂H & OH) radicals coupled with nanoparticles of titanium compounds. *Fuel*, **180**, 218-227 (2016).
- 11) M. H. Habibi, H. Vosooghian, photocatalytic degradation of some organic sulfides as environmental pollutants using titanium dioxide suspension. *Chem.*, **174**, 45-52 (2005).

- 12) J. Zhang, D. S. Zhao, J. L. Wang, L. Y. Yang, Photocatalytic oxidation of dibenzothiophene using TiO₂/bamboo.Charcoal. *Sci.*, **44**, 3112–3117 (2009).
- 13) S. Matsuzawa, J. Tanaka, S. Sato, T. Ibusuki, Photocatalytic oxidation of dibenzothiophenes in acetonitrile using TiO₂: effect of hydrogen peroxide and ultrasound irradiation. *Chem.*, **149**, 183–189 (2002).
- 14) X. Wang, K. [Maeda](#), A. [Thomas](#), K. [Takanabe](#), G. [Xin](#), J. M. [Carlsson](#), K. Domen, M. Antonietti, A metal-free polymeric photocatalyst for hydrogen production from water under visible light. *Nature Mater*, **8**, 76–80 (2009).
- 15) B. Muktha, G. Madras, T. N. Guru Row, U. Scherf, S. Patil, Conjugated polymers for photocatalysis. *Phys. Chem.*, **B 111**, 7994–7998 (2007).
- 16) Q. Luo, L. Bao, D. Wang, X. Li, J. An, Preparation and strongly enhanced visible light photocatalytic activity of TiO₂ nanoparticles modified by conjugated derivatives of polyisoprene. *Phys. Chem.*, **C 116**, 25806–25815 (2012).
- 17) M. Zhang, W. D. Rouch, R. D. McCulla, Conjugated polymers as photoredox catalysts: Visible-light-driven reduction of aryl aldehydes by poly(p-phenylene). *Eur. J. Org. Chem.*, 6187–6196 (2012).
- 18) A. B. Al-Sayed, H. I. Al-Shafey, E. I. Arafa, A. M. A. El Naggar, Synthesis and characterization of polymerized acrylamide coupled with acrylamido-2-methyl-1-propane sulfonic acid-montmorillonite structure as novel nano-composite for Cd (II) removal from aqueous solutions. *ACS chemical & Engineering Data*, **65**, 4079-4091 (2020).
- 19) A. M. A. El Naggar, M. M. Ali, S. A. Abdel-Maksoud, M. H. Taha, A. A. Elzoghby, Waste generated bio-char supported co-nanoparticles of nickel and cobalt oxides for efficient adsorption of uranium and organic pollutants from industrial phosphoric acid. *Radioanalytical and Nuclear chemistry*, **320**(3), 741-755(2019).
- 20) M. M. Ali, S. A. Abdel-Maksoud, [M. H. Taha](#), A. M. A. El Naggar, [A. S. Morshedy](#), [A. A. Elzoghby](#), Uranium separation from phosphoric acid using metallic carbonaceous structures as efficient adsorbents: an experimental and kinetic study. *Radiochemistry Journal*, **62** (2), 204-216 (2020).
- 21) A. M. A. El Naggar, C. Kazak, Preparation and characterization of novel nano-structured porous nickel alloy composite induced by electroless deposition and its performance in the hydrogen separation. *Separation and purification technology*, **160**, 73-80 (2016).
- 22) A. M. A. El Naggar, G. Akay, Novel Intensified Catalytic Nano-Structured Nickel-Zirconia Supported Palladium Based Membrane for High Temperature Hydrogen Production from Biomass Generated Syngas. *International Journal of Hydrogen Energy*, **38** (16), 6618-32 (2013).
- 23) A. M. A. El Naggar, M. Noor El-Din, M. R. Mishrif, I. M. Nassar, Highly efficient Nano-Structured polymer based membrane/sorbent for oil removal from O/W emulsion conducted of petroleum wastewater. *Dispersion science and technology*, **36**, (1), 118-128 (2015).
- 24) A. M. A. El Naggar, H. M. Gobara, H. A. El Sayed, F. S. Soliman, New Advances in Hydrogen Production via the Catalytic Decomposition of Wax By-Products Using Nanoparticles of SBA Frame-worked MoO₃. *Energy Conversion and Management*, **106**, 615-624 (2015).
- 25) D. R. Abd El-Hafiz, S. A. El-Temtamy, M. A. Ebiad, R. A. El-Salamony, S. A. Ghoniem, A. M. A. El Naggar, T. S. Gendy, Novel La Ni Intercalated Egyptian Bentonite Clay for Direct Conversion of Methane Using CO₂ as Soft Oxidant. *International Journal of hydrogen energy*, **45** (16), 9783-9794 (2020).
- 26) H. A. Elwan, A. S. Morshedy, A. M. A. El Naggar, [Highly Efficient Visible-Light-Induced Photocatalytic Hydrogen Production via Water Splitting using FeCl₃-Based Ionic Liquids as Homogeneous Photocatalysts](#). *ChemSusChem* (Wiley online), **13** (24), 6602-6612 (2020).
- 27) R. S. Mohamed, A. A. Al Kahlawy, A. M. A. El Naggar, H. M. Gobara, Innovative approach for production of carbon nanotubes (CNTs) and carbon nano-sheets through highly efficient photocatalytic water splitting into hydrogen using metal organic frameworks (MOF)-nano TiO₂ matrix as novel catalyst. *New Journal of Chemistry-RSC*, **44**, 5097-5108 (2020).
- 28) A. M. A. El Naggar, M. S. Darwish, A. S. Morshedy, Nanomaterials for hydrogen production through photocatalysis. *Energy*,

- Environmental and sustainability, 251-273 (2019).
- 29) N. H. [Shalaby](#), R. A. [Elsalamony](#), A. M. A. [El Nagggar](#), [Mesoporous waste-extracted SiO₂-Al₂O₃-supported Ni and Ni-H₃PW₁₂O₄₀ nano-catalysts for photo-degradation of methyl orange dye under UV irradiatio](#). [New Journal of Chemistry](#), **42**(11), 9177-9186 (2018).
- 30) H. M. Gobara, I. M. Nassar, A. M. A. El Nagggar, G. Eshaq, Nanocrystalline Spinel Ferrite for an Enriched Production of Hydrogen through a Solar Energy Stimulated Water Splitting Process. *Energy Journal*, **118**, 1234-1242 (2017).
- 31) A. S. Morshedy, H. M. Abd El Salam, A. M. A. El Nagggar, T. Zaki, Hydrogen production and in-situ storage through process of water splitting using mono/ binary metal-organic framework (MOF) structures as new chief photocatalysts. *Energy & Fuels (ACS)*, **34** (9), 11660-11669 (2020).
- 32) M. S Darwish, A. M. A El Nagggar, A. S Morshedy, N. Haneklaus, Increased production of hydrogen with in-situ CO₂ capture through the process of water splitting using magnetic core/shell structures as novel photocatalysts. *Environmental science and pollution research*, **28** (3), 3566-3578 (2021).
- 33) A. M. A. ElNagggar, H. M. Gobara, I. M. Nassar, Novel nanostructured for the improvement of hydrogen production from water splitting via a photo-catalyzed reaction with in-situ nanocarbons formation. *Renewable and Sustainable Energy Reviews*, **41**, 1205–1216 (2015).
- 34) A. M. A. El Nagggar, I. M. Nassar, H. M. Gobara, Enhanced hydrogen production from water via a photo-catalyzed reaction using chalcogenide d-element nanoparticles induced by UV light. *Nanoscale*, **5**(20), 9994-9999 (2013).
- 35) A. S. Morshedy, A. M. A. El Nagggar, S. M. Tawfik, O. I. Sif El-Din, S. I. Hassan, A. I. Hashem, [Preparation and characterization of micro-porous ZnO nanoparticles](#). *Egyptian Journal of Chemistry*, **59**(4), 609-621 (2016).
- 36) A. S. Morshedy, A. M. A. El Nagggar, S. M. Tawfik, O. I. Sif El-Din, S. I. Hassan, A. I. Hashem, Photo-Assisted Desulfurization Induced by Visible Light Irradiation for the Production of Ultra-Low Sulfur Diesel Fuel Using Nanoparticles of CdO. *Physical Chemistry (ACS)*, **120** (46), 26350-26362 (2016).
- 37) M. S. Mostafa, A. A. Bakr, A. M. A. El Nagggar, E. A. Sultan, Water decontamination via the removal of Pb (II) using a new generation of highly energetic surface nano-material: Co⁺²Mo⁺⁶ LDH. *Colloid and interface science*, **461**, 261-272 (2016).
- 38) A. G. Soliman, A. M. A. El Nagggar, M. R. Noor El-Din, A. M. Ramadan, M. A. Youssef, Optimization of dosing and mixing time through fabrication of high internal phase emulsion (HIPE) polymerization based adsorbents for use in purification of oil in water contaminated wastewater. *Journal of applied polymer science*, Wiley online, **137** (34), 1-11 (2020).